ACS APPLIED MATERIALS & INTERFACES

Research Article

www.acsami.org

Exploring and Exploiting Dynamic Noncovalent Chemistry for Effective Surface Modification of Nanoscale Metal–Organic Frameworks

Shuo Liu, Linxiang Zhai, Chunxiang Li, Yujie Li, Xiangqun Guo, Yibing Zhao, and Chuanliu Wu*

The MOE Key Laboratory of Spectrochemical Analysis and Instrumentation, State Key Laboratory of Physical Chemistry of Solid Surfaces, Department of Chemistry, College of Chemistry and Chemical Engineering, Xiamen University, Xiamen, 361005, P. R. China

Supporting Information

ABSTRACT: Surface properties determine, to a great extent, the biologically relevant functions of various kinds of nanosized materials. Although the modification of the surface of traditional inorganic or polymeric nanoparticles can be routinely achieved through covalent or noncovalent manner or both, the surface modification of nanoscale metal–organic frameworks (nano-MOFs) is extremely challenging because of their rapid degradation in aqueous environments. In this work, we systematically studied the synergistic and dynamic noncovalent interactions between fluorescent probes and iron(III) carboxylate nano-MOFs (i.e., MIL-101-NH_2 (Fe), one of the most prevalent MOFs used in drug delivery and imaging). We further examined the interplay between the surface binding of fluorescent probes and the degradation of MIL-101-NH_2 (Fe) in aqueous medium. It was demonstrated that the surface binding of probes is not only of high affinity but also dynamic and nonsheddable, even during the degradation, a feature that is essentially different from the covalent conjugation. Subsequently, we developed a unique and straightforward strategy for the surface modification of MIL-101-NH_2 (Fe) with polymer by exploiting the synergy of noncovalent interactions between functionalized copolymers and MIL-101-NH_2 (Fe). We demonstrated that the binding of polymers onto MIL-101-NH_2 (Fe) surface was very effective in aqueous solution and surprisingly nonsheddable during the process of degradation. Surface polymers can creep on the surface of MIL-101-NH_2 (Fe), in a dynamic and real-time manner, to the new sites formed immediately after the degradation. In addition, the stability of MIL-101-NH_2 (Fe) particles in aqueous environments can be improved to some extent by the surface polymer coating. The results presented herein constitute an important innovation for surface engineering of nano-MOFs, which would benefit the application of nano-MOFs as delivery systems in aqueous systems.

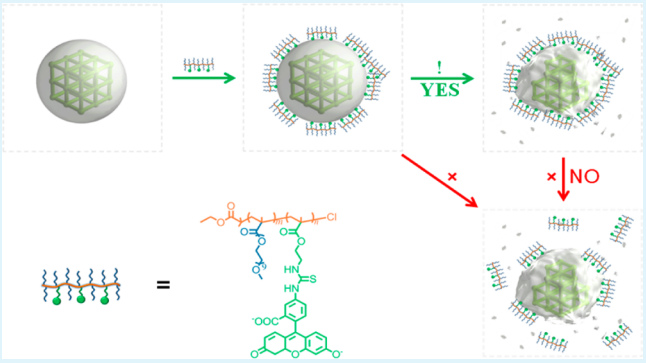

KEYWORDS: *dynamic noncovalent chemistry, metal–organic framework, surface modification, polymer, fluorescent probe*

INTRODUCTION

Metal–organic frameworks (MOFs), also known as coordination polymers, are the latest class of crystalline porous materials,[1−3] which have been of considerable interest for many potential applications.[4−11] The use of MOFs in biomedicine is constantly emerging because of their intrinsic advantages in drug delivery and imaging applications compared to traditional carriers such as organic polymers and inorganic materials.[12−15] For example, the composition, structure, and pore size of MOFs can be easily tuned through changing of the metal and/or organic building blocks.[16,17] Another key advantage is the biodegradability, a characteristic that would dramatically reduce their toxicity and potential risk of long-term accumulation in tissues.[14,15,18,19] In many biomedical applications, MOFs have been frequently engineered as nanoparticles (nano-MOFs) to improve their imaging and therapeutic efficacies. For instance, Horcajada et al. have recently reported that porous iron(III) carboxylate nano-MOFs can serve as superior carriers for efficient drug delivery and imaging applications.[15] They also demonstrated that this kind of nano-MOF was nontoxic in vitro because of their intrinsic biodegradable character. More recently, Baati et al. have further proved a low in vivo acute toxicity of porous iron(III) carboxylate nano-MOFs.[20]

Although the degradation of MOFs brings much benefit, it does cause troubles. First of all, it leads to difficulties in permanently modifying the surface of nano-MOFs to confer unique surface functions,[13] a modification that has been demonstrated to be important for the improvement of therapeutic efficacy of various nanomaterials.[21−23] It is argued

Received: July 30, 2013
Accepted: April 3, 2014
Published: April 3, 2014

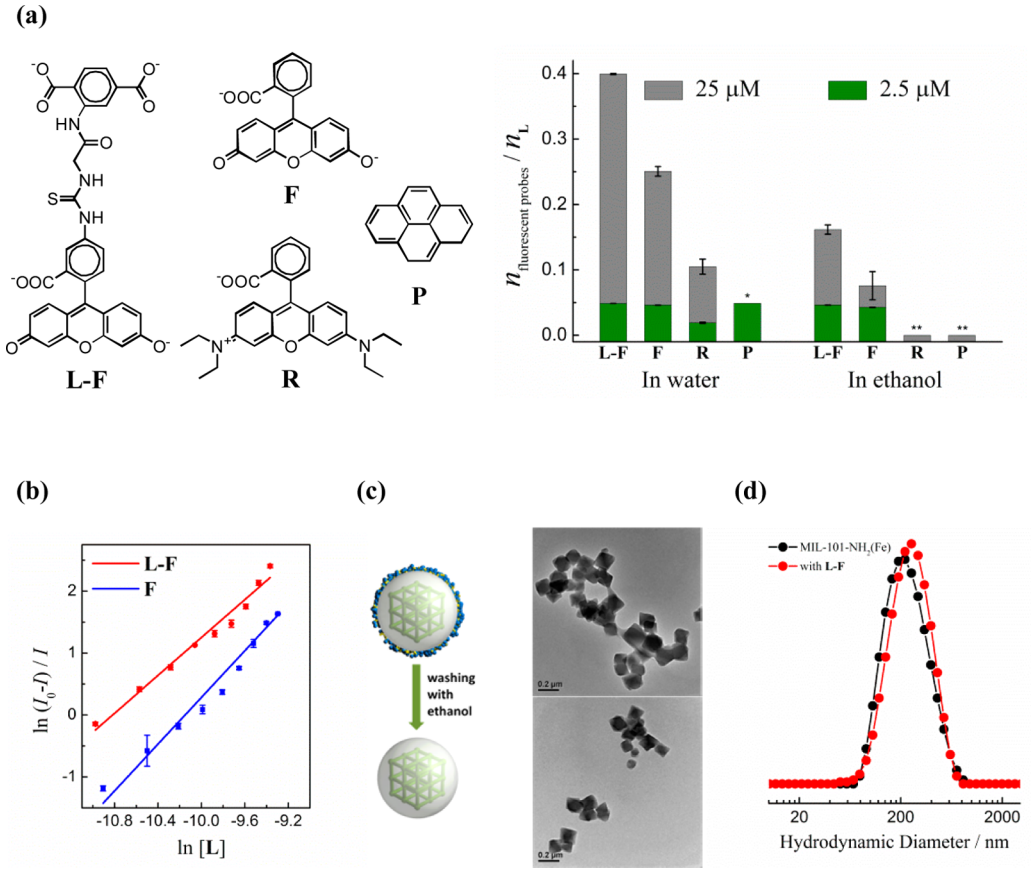

Figure 1. (a) Structures of fluorescent probes (**L-F**, **F**, **R**, and **P**), and the binding efficiency of fluorescent probes onto MIL-101-NH_2 (Fe) surface in water and that in ethanol, as determined by the molar ratio of probes to organic building block (**L**) of MIL-101-NH_2 (Fe) in precipitates after incubation with two different concentrations of probes (2.5 and 25 μM). ∗ denotes not determined at 25 μM because of its low solubility. ∗∗ denotes no binding of probes observed. Data are presented as the mean ± SD (n = 3). (b) Plots of binding efficiency of **L-F**/**F** onto MIL-101-NH_2 (Fe) versus the concentration of **L**, which were fitted by Hill equation (solid line); mean ± SD (n = 3). (c) TEM image of **L-F** bound MIL-101-NH_2 (Fe) (top) and that after washing with ethanol (bottom); corresponding diagrams were shown in the left side. (d) Size distribution of MIL-101-NH_2 (Fe) with (red line, polydispersity index (PDI) = 0.151) and without (black line, PDI = 0.198) surface bound/assembled **L-F** determined by DLS.

that modifying the surface of nano-MOFs with polymers or functional molecules through covalent conjugation should be extremely ineffective because the linked conjugates would shed steadily from the particle surface because of the gradual degradation of the matrix in aqueous environments. In addition, it is possible that porous solids such as MOFs may not degrade from the outer to the inner part of the particles but more likely they break from the inside because water (or hydroxide ions) can diffuse easily through the pores. In this context, covalent modifications on the surface of nano-MOFs might be expected to be, to some extent, stable throughout the degradation process. In spite of this, thus far the most investigated route for the surface modification of nano-MOFs has been to exploit the noncovalent binding of molecules such as lipids and polymers onto the nano-MOFs surface.[24−28] However, systematic understanding of the detailed mechanism of noncovalent binding is still extremely lacking. Secondly, the degradation of MOFs also leads to difficulties in maintaining the stability and dispersity of nano-MOFs in aqueous environments. Although this issue may be overcome, to some extent, by postsynthetic modification of nano-MOFs with a thin inorganic layer such as silica,[14,29−33] a new issue regarding the biocompatibility of the surface inorganic solids subsequently arises. An alternative strategy to consolidate nano-MOFs relies on choosing appropriate metals and/or organic linkers or through synthetic modification of networks, which however is far from realistic. To our knowledge, even the most robust MOFs still suffer from poor stability in aqueous solution[34] and are not tolerant to pH variation. In particular, most nano-MOFs materials are extremely unstable under physiological pH and ionic conditions.

In this work, we systematically explored the synergistic noncovalent interactions on the surface of iron(III) carboxylate nano-MOFs, MIL-101-NH_2 (Fe), which is one of the most prevalent MOFs used in drug delivery and imaging, by strategically exploiting designed fluorescent dyes as probes. The dynamic process of the surface molecular binding/assembly and the degradation of MIL-101-NH_2 (Fe) in aqueous medium were also studied. After that, a unique and straightforward strategy that exploits the multiple, synergistic, and dynamic noncovalent interactions between functionalized comb-shaped copolymers and MIL-101-NH_2 (Fe) was developed for the surface modification of MIL-101-NH_2 (Fe). The binding of polymers onto MIL-101-NH_2 (Fe) surface was demonstrated to be not only very effective but also surprisingly nonsheddable, even during the process of degradation. In addition, the surface polymer coating was also found to be able to improve, to some extent, the stability of MIL-101-NH_2 (Fe) particles in aqueous environments.

dx.doi.org/10.1021/am500192b | ACS Appl. Mater. Interfaces 2014, 6, 5404−5412

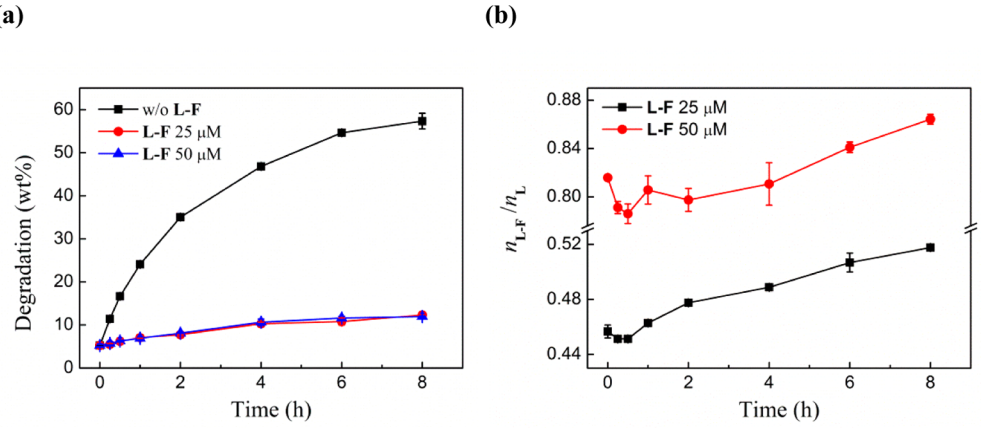

Figure 2. (a) Kinetics of degradation of MIL-101-NH_2 (Fe) (0.01 mg/mL, black) and that in the presence of 25 μM (red) and 50 μM (blue) of **L-F** in aqueous solution. (b) Evolution profile of the content of surface bound/assembled **L-F** (determined by the molar ratio of **L-F** to **L** in precipitates obtained through centrifugation) as the degradation of MIL-101-NH_2 (Fe) proceeded in water. Concentration of **L-F** in solutions were 25 μM (black) and 50 μM (red). Data are presented as the mean ± SD (n = 3).

RESULTS AND DISCUSSION

Synergy of Noncovalent Interactions. MIL-101-NH_2 (Fe) was synthesized by the reaction of equimolar amounts of $FeCl_3$ and 2-aminoterephthalic acid (**L**) in aqueous medium under microwave heating.[15] The size, shape, and structure of the resulting particles were analyzed by transmission and scanning electron microscopy (TEM and SEM), powder X-ray diffraction (PXRD), thermogravimetric analysis (TGA), nitrogen adsorption study, dynamic light scattering (DLS), and ζ-potential measurement (Figures S1−S5). MIL-101-NH_2 (Fe) exhibits an octahedral morphology and an average diameter of around 184 nm. PXRD indicates that the obtained particles are crystalline and of the same structure as the reported MIL-101-NH_2 (Fe) samples.[14,35] The ζ-potential of MIL-101-NH_2 (Fe) surface was measured to be approximately +38 mV under neutral aqueous condition (pH ≈ 7). The positive surface charges are likely derived from the metal centers and/or the protonation of the amino group of **L**.

A fluorescent probe (**L-F**) was synthesized through the conjugation of **L** and fluorescein (**F**) with a short molecular linker (structure shown in Figure 1a). We can speculate that MIL-101-NH_2 (Fe) surface bearing positive charges, hydrophobic channels, and open metal sites would exhibit strong binding capability to **L-F** due to the synergy of surface electrostatic/hydrophobic interactions and coordination of **L-F** with metal centers. Thus, the binding of **L-F** with MIL-101-NH_2 (Fe) was analyzed in several different manners and compared with that of **F** and other probes (rhodamine b, **R**; pyrene, **P**). After incubation of fluorescent probes with MIL-101-NH_2 (Fe) in water (and in ethanol) for 15 min, the particles were precipitated by centrifugation. The concentrations of fluorescent probes in the suspension and precipitate were determined respectively by fluorescence after digesting the samples with phosphate buffer (pH 7.4). Figure 1a shows the binding efficiency of MIL-101-NH_2 (Fe) toward different fluorescent probes in water (and in ethanol). We observed that MIL-101-NH_2 (Fe) exhibits strong binding strength to all fluorescent probes in water, while in ethanol it only binds **L-F** and **F**. In contrast to **R** and **P**, both **L-F** and **F** are negatively charged. This finding, therefore, strongly indicates the essential contribution of electrostatic attraction between **L-F**/**F** (i.e., **L-F** or **F**) and MIL-101-NH_2 (Fe) or coordination of **L-F** with metal centers to the binding event. In addition, the binding of **R** or **P** to MIL-101-NH_2 (Fe) in water was much more efficient than that in ethanol, stressing the contribution of hydrophobic interactions to the strong binding of fluorescent probes to MIL-101-NH_2 (Fe) in aqueous solution. Whether in water or in ethanol, the binding efficiency of MIL-101-NH_2 (Fe) toward **L-F** was superior to that for other probes, and the difference in efficiency became more pronounced if the precipitates were washed several times with ethanol (Figure S6). Taken together, these results have clearly demonstrated the importance of exploring the synergy of noncovalent interactions in achieving strong binding of molecules to MIL-101-NH_2 (Fe) materials. In addition, considering that MIL-101-NH_2 (Fe) particles possess a cationic framework and as the **L-F** and **F** molecules are anionic molecules, it is likely that a partial anion exchange of the constitutive linkers (**L**) by the **L-F** or **F** molecules or a direct grafting of the molecules through the Lewis acid sites of the MIL-101-NH_2 (Fe) also plays important roles in the binding processes.[36−38] However, by monitoring the amount of **L** released into solution after the binding of **L-F** or **F**, we have proved that the anion exchange process should be negligible (~3−5% of **L** in MIL-101-NH_2 (Fe) particles was released by anion exchange) if **L** can efficiently diffuse into the solution after the exchange.

To further explore the mechanism of binding of **L-F**/**F** to MIL-101-NH_2 (Fe), the degree of cooperativity of the binding process was evaluated through measurement of the Hill coefficient n (see Supporting Information for details).[39−42] Figure 1b shows Hill plots associated with the measurements of binding efficiency between **L-F**/**F** and MIL-101-NH_2 (Fe). The Hill coefficient of the binding can then be obtained from the slope of the plots. Interestingly, we observed positively cooperative binding for both probes (n>1), which indicates that their binding affinity to MIL-101-NH_2 (Fe) becomes progressively stronger as more molecules adsorbed. The observed positive cooperativity should arise from the synergistic enhancement of hydrophobic interactions between probe molecules on the surface (or in the pores) of MIL-101-NH_2 (Fe). The relatively lower degree of cooperativity for **L-F** (n = 1.52) compared to that for **F** (n = 1.89) reveals that the intermolecular electrostatic repulsion between **L-F** molecules very likely has a negative effect on the cooperative binding process. To our knowledge, this is the first reported case of showing the positively cooperative binding of small molecules to nano-MOFs.

dx.doi.org/10.1021/am500192b | ACS Appl. Mater. Interfaces 2014, 6, 5404−5412

Further analyses suggest that a considerable amount of probe molecules were assembled on the surface of MIL-101-NH_2 (Fe). We observed a thin and misty layer of matter on the particle surface from TEM images in Figure 1c, a layer that can be destroyed immediately by washing with ethanol, thus providing strong evidence of the formation of surface hydrophobic assemblies. The framework morphology (Figure 1c) and crystalline structure (Figure S2) were not significantly changed after the binding or detaching of probes. In addition, nitrogen isotherms of MIL-101-NH_2 (Fe) samples reveal that the BET surface area was slightly increased from 1945 to 2379 m^2/g after the binding of **F** (Figure S4), but the average pore sizes remain nearly unchanged (2.8 nm before **F** binding versus 2.7 nm after **F** binding). The observed increase in surface area is unexpected, probably reflecting a contribution of the adsorbed **F** on the nitrogen adsorption. Furthermore, we also observed a slight increase of the hydrodynamic diameter (Figure 1d) after the binding of **L-F**, together with a shift of the surface ζ-potential from +38 to +28 mV (Figure S7). These findings, in combination with the preceding data, have strong implication that probe molecules can effectively bind and assemble on the surface of MIL-101-NH_2 (Fe) through synergistic noncovalent interactions and a process of cooperative binding, though there is still no strong evidence to rule out the possibility of the entering of **L-F**/**F** into the pores of MIL-101-NH_2 (Fe) particles.

Dynamic Process of Binding. The degradability of nano-MOFs in aqueous environments is one of the most attractive merits for their application in biomedicine. It was found that the degradation of free MIL-101-NH_2 (Fe) occurred immediately when dispersed in water (pH ~7), and after 8 h, around 50 wt % of particles were completely decomposed (Figure 2a). DLS analysis shows that the hydrodynamic diameter of MIL-101-NH_2 (Fe) decreased slightly from ~200 to 190 nm as the degradation proceeded to 30 wt % (Figure S8). Further degradation results in a remarkable increase in the hydrodynamic diameter probably due to the formation of particle agglomerates. In addition, TEM images show an increase in the surface roughness of the particles in the early stage of degradation (Figure S9), a result that was consistent with the decrease of hydrodynamic diameter obtained by DLS.

We further examined the interplay between the degradation of MIL-101-NH_2 (Fe) in aqueous solution and the binding/assembly of probe molecules on the surface of particles. Interestingly, we observed that the surface bound fluorescent probes could significantly slow the degradation process of MIL-101-NH_2 (Fe) (Figure 2a). In an aqueous solution of **L-F** (25 or 50 μM, pH ≈ 7) or **F** (Figure S10), less than 7 wt % of MIL-101-NH_2 (Fe) particles were degraded after 8 h, which was significantly lower than that of free particles. Considering that the binding of **F**/**L-F** leads to a formation of hydrophobic assemblies on the particle surface, such an increase in stability is very likely caused by the decrease in the diffusion of water into the pores. Moreover, what struck us is that the content of the surface bound probes obviously increased as MIL-101-NH_2 (Fe) decomposed with time (Figure 2b). Even if the surface assembled layer of probes was removed by washing with ethanol, the residual probes that were tightly bound to MIL-101-NH_2 (Fe) were still found to be extremely nonsheddable as the degradation proceeded (Figure S11). It is plausible that probe molecules that are ultimately released from the decomposed MIL-101-NH_2 (Fe) can immediately redistribute and bind to other particles. Thus, the binding of probe molecules to nano-MOFs via synergistic noncovalent interactions is not only of high affinity but also dynamic and nonsheddable, even in degradation, a feature that could be essentially different from the covalent conjugation. It is argued that strong noncovalent interactions between guest molecules (**L-F** or **F**) and particle surface would result in the aggregation of particles due to interparticle interactions mediated by guest molecules. This was not observed, very likely owing to fact that the surface ζ-potential of particles is still positive enough (shift from +38 to +28 mV) after the binding of guest molecules.

Finally, we examined if the binding of **F** affects the accessibility of the pores of MIL-101-NH_2 (Fe) particles to small molecules such as caffeine. We found that the loading capacities of caffeine were not significantly changed before and after the binding of **F** (Figure S12), indicating the negligible effect of the surface binding of **F** on the accessibility of pores. After that, we further explored the effect of the surface **F** adsorption on the kinetics of the release of caffeine molecules. The result shows that the loaded caffeine can be completely released as soon as the particles were dispersed in aqueous solution, and the binding of **F** does not obviously change the release process (Figure S12). This finding suggests that the noncovalent (predominantly hydrophobic) interactions between caffeine and MIL-101-NH_2 (Fe) frameworks should be extremely weak, as a consequence that the surface binding of **F** and the subsequent improvement in the stability of MIL-101-NH_2 (Fe) in aqueous solution impart no remarkable effect on the retention of caffeine molecules in MIL-101-NH_2 (Fe) pores. In addition, we observed that the surface-bound **F** molecules were still extremely nonsheddable as the caffeine was released from MIL-101-NH_2 (Fe) pores to aqueous solution (Figure S12).

Surface Polymer Modification. In light of the strong binding strength between negatively charged/hydrophobic molecules (**L-F**, **F**) and MIL-101-NH_2 (Fe), we further explored the possibility of exploiting the synergy of dynamic noncovalent interactions for modifying the surface of nano-MOFs with polymers. Three different copolymers (**Poly-F-1**, **Poly-F-2**, and **Poly-F-3**) bearing poly(oligoethylene glycol monomethyl ether methacrylate) (pOEGMA) backbone and different ratios of poly(2-aminoethyl methacrylate) (pAEMA) conjugated with **F** as binding moiety were synthesized,[43] the structures of which are shown in Scheme 1a; their detailed characterizations are given in Supporting Information (Figure S13 and Tables S1 and S2). pOEGMA is an emerging comb-shaped derivative of polyethylene glycol that possesses unique biocompatibility which has been used for surface modification of various materials.[43−48]

The binding of **Poly-F-1/2/3** (i.e., **Poly-F-1**, **Poly-F-2**, or **Poly-F-3**) to MIL-101-NH_2 (Fe) was evaluated by incubating a certain amount of MIL-101-NH_2 (Fe) (0.04 mg/mL) with different concentrations of polymers in water, which was followed by measuring the amount of polymers in precipitates and/or in suspensions after centrifugation. Figure 3a shows that the amount of **Poly-F-1/2/3** adsorbed on MIL-101-NH_2 (Fe) surface initially increases rapidly with concentration, the trend of increase that either reaches a plateau (**Poly-F-1**) or significantly slows (**Poly-F-2/3**) at higher concentrations. It was demonstrated that the relative content of side chain **F** in polymers has a marked effect on the binding behavior (discussed in Supporting Information). In addition, we observed that **Poly-F-1/2/3** in water can bind completely to MIL-101-NH_2 (Fe) surface at lower concentrations (Figure 3a), signifying a superhigh binding affinity. The binding efficiency of MIL-101-NH_2 (Fe) toward **Poly-F-1/2/3** approaches ~100% at lower concentrations; further increase in the concentration leads to a saturation of

Scheme 1. (a) Structure of pOEGMA/pAEMA Copolymer–Fluorescein Conjugates[a] and (b) Diagram Illustrating the Binding/Assembly of Polymers onto the Surface of MIL-101-NH_2 (Fe)[b]

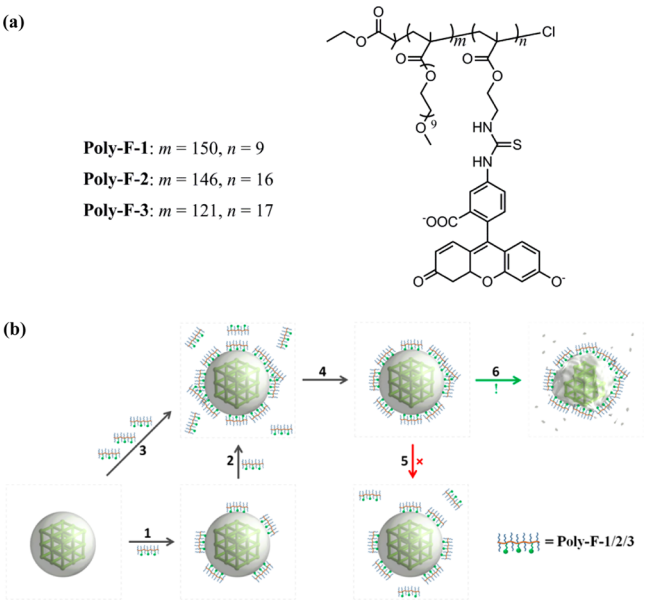

[a] m = average number of OEGMA units, n = average number of side chain **F**. The segment of free AEMA units was omitted for clarification. [b] Routes 1–3: different concentrations of polymers incubated. Route 4: free polymers removed by centrifugation. Route 5: dissociation of polymer from the surface (not observed). Route 6: degradation of MIL-101-NH_2 (Fe) and redistribution of surface polymers.

surface binding (Scheme 1b, routes 1–3). Importantly, we found that the binding of polymers to MIL-101-NH_2 (Fe) is surprisingly nonsheddable (Figure 3b). That is, even when the free polymers in solution were completely removed by repeated centrifugal washing, the bound polymers still adhere well on the particle surface instead of redistributing and diffusing into solution (Scheme 1b, routes 4 and 5), a feature which should be of crucial importance to the effective and quasi-permanent surface modification. The successful modification of polymers on the particle surface was also confirmed by using infrared (IR) absorption spectroscopy (Figure S14) and TGA (Figure S3). We observed that MIL-101-NH_2 (Fe) particles modified with polymers exhibit typical IR absorption peaks from pOEGMA/pAEMA copolymers. This sample had a polymer loading (**Poly-F-2**) of 30.2% by TGA. Furthermore, we demonstrated that control polymers (without side chain **F**) exhibit negligible binding efficiency (Figure 3c and Figure S15), indicating that noncovalent interactions mediated by **F** moieties are the predominant driving force contributing to the binding event.

To obtain the grafting density of the polymers on the surface of MIL-101-NH_2 (Fe) particles, we first have to assume that the density of MIL-101-NH_2 (Fe) particles is equal to that of bulky MIL-101-NH_2 (Fe), which can be calculated to be 0.617 g/cm^3 based on its crystal structure. The MIL-101-NH_2 (Fe) particles were roughly spherical and had an average diameter of about 184 nm by TEM (Figure S1). Thus, we can obtain that one particle had a weight of 2.0×10^{-12} mg and an external surface area of 1.06×10^5 nm^2. By using these parameters, we can then obtain from Figure 3b that the grafting density of polymers was 0.20, 0.18, and 0.20 polymer chains per nm^2 on the surface of MIL-101-NH_2 (Fe) after five-round washing with water for **Poly-F-1**, **Poly-F-2**, and **Poly-F-3**, respectively.

DLS data show that the monodispersity of MIL-101-NH_2 (Fe) particles remains unchanged after the polymer modification, thus ruling out the possibility of forming cross-linkages of particles through polymer bridges (Figure S16). In addition, an increase in the hydrodynamic diameter, together with a marked shift of the surface ζ-potential to negative direction, unambiguously confirmed the formation of polymer coatings on the particle surface. TEM images indicate no change in the morphology of MIL-101-NH_2 (Fe) after polymer coating (Figure S17).

It was most interesting to discover that surface polymers are surprisingly nonsheddable during the degradation (Scheme 1b, route 6). As the degradation of polymer-modified MIL-101-NH_2 (Fe) proceeded in water, the amount of the surface-adsorbed polymers remains constant (or slightly increases if the free polymers in solutions were not removed, likely because of the increase of surface areas along with the degradation) (Figure 4a). It should be conceivable that the surface polymers could creep on the surface of MIL-101-NH_2 (Fe), in a dynamic and real-time manner, to the new sites formed immediately after the degradation by exploiting the multiple and dynamic noncovalent interactions between polymer and MIL-101-NH_2 (Fe) surface. In addition, we observed that surface polymers can markedly slow the kinetics of the degradation of MIL-101-NH_2 (Fe) in water (Figure 4b). We have demonstrated that polymers on the particle surface were not only of high affinity but of high grafting density (0.18–0.20 polymer chains per nm^2). In addition, we observed that side chain **F** in different polymer chains had a cooperative effect ($n > 1$, Hill plots in Figure S13) on the binding process due to the hydrophobic interaction of side chain **F**. Thus, the decrease in the degradation rate resulting from polymer grafting arises very likely from the decrease of the diffusion of water into the pores of particles by surface grafted polymers which strongly prevent the reaction between MIL-101-NH_2 (Fe) framework and water molecules (or hydroxide ions). DLS analysis further points to the influence of surface polymer coatings on the protection of MIL-101-NH_2 (Fe) from forming agglomerates during the process of degradation. No aggregation of polymer-coated MIL-101-NH_2 (Fe) particles was detected during the degradation in contrast to what happened in aqueous solution of particles without surface polymer coating (Figure S18).

GENERAL DISCUSSION

The surface morphology and properties of traditional inorganic or polymeric nanoparticles are usually considerably stable, which lends facility for modifying the surface with unique functions in a noncovalent or covalent manner or both.[49−53] Nano-MOFs that contrast significantly with these nanoparticles, however, suffer from poor surface stability, which nearly excludes the possibility of modifying the surface effectively through covalent conjugation. In this context, the dynamic feature of noncovalent interactions appears very promising for the development of novel strategies for surface engineering of nano-MOFs. Although there are documented instances where small molecular drugs, enzymes, lipids, and polymers can be encapsulated in the pores or adsorbed on the surfaces of nano-MOFs,[15,24−28,36,37,54] systematic understanding of the detailed mechanism of binding that involves, as discussed in this work, synergy of noncovalent interactions, cooperative binding behaviors, and dynamic features of surface coating associated with degradation is still extremely lacking. In light of the findings herein, noncovalent

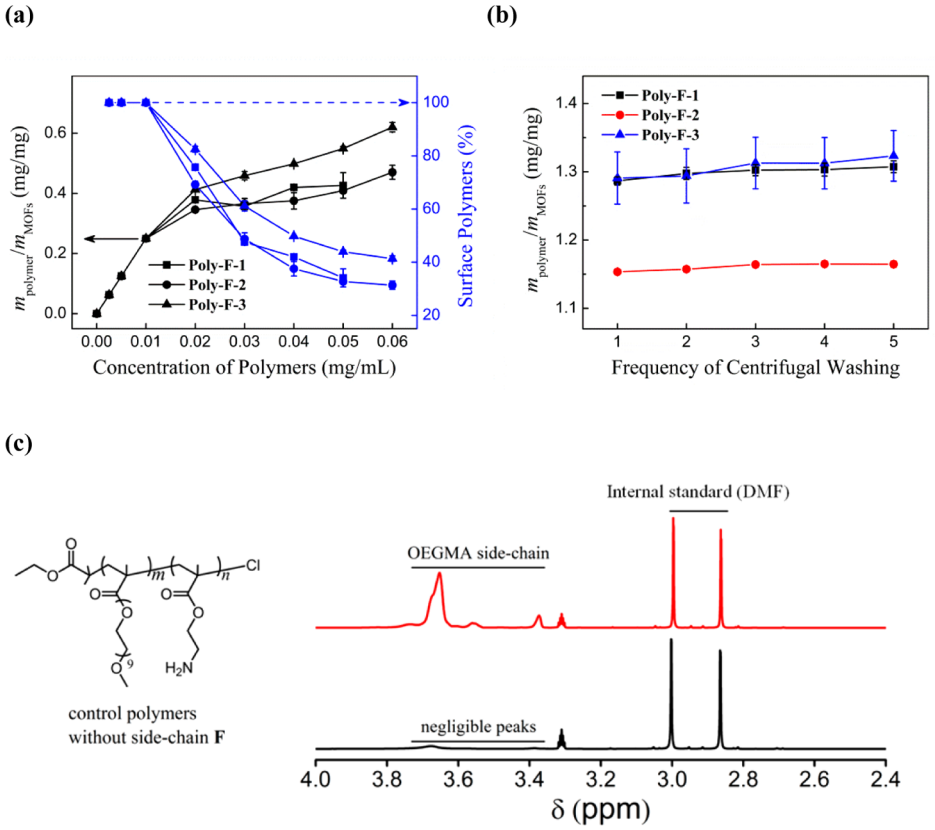

Figure 3. (a) Amount of the polymers bound/assembled on the surface of MIL-101-NH_2 (Fe) (0.04 mg/mL) in water as the concentration of **Poly-F-1/2/3** increased, determined by mass ratio of polymer to MIL-101-NH_2 (Fe) in precipitates obtained through centrifugation (left, black) and by the percentage of surface-adsorbed polymer in total polymer present both on the surface and in the solution (right, blue). (b) Evolution profile of the content of **Poly-F-1/2/3** adsorbed on the surface of MIL-101-NH_2 (Fe) (0.04 mg/mL) upon washing with water several times, determined by mass ratio of surface-bound polymer to MIL-101-NH_2 (Fe). Original polymer concentration in solution was 0.5 mg/mL. Data are presented as the mean ± SD (n = 3). (c) Representative ^{1}H NMR analysis indicates a negligible amount of control polymers (herein is the homologue of **Poly-F-1**; i.e., **Poly-1**) adsorbed on the surface of MIL-101-NH_2 (Fe), as determined by comparing the peak intensity of pOEGMA (black line) on the surface of MIL-101-NH_2 (Fe) with that of pure polymer (red line) of equal amount that was used for the binding experiment (i.e., indicative of 100% adsorption). Dimethylformamide (DMF) was strategically added as internal standard.

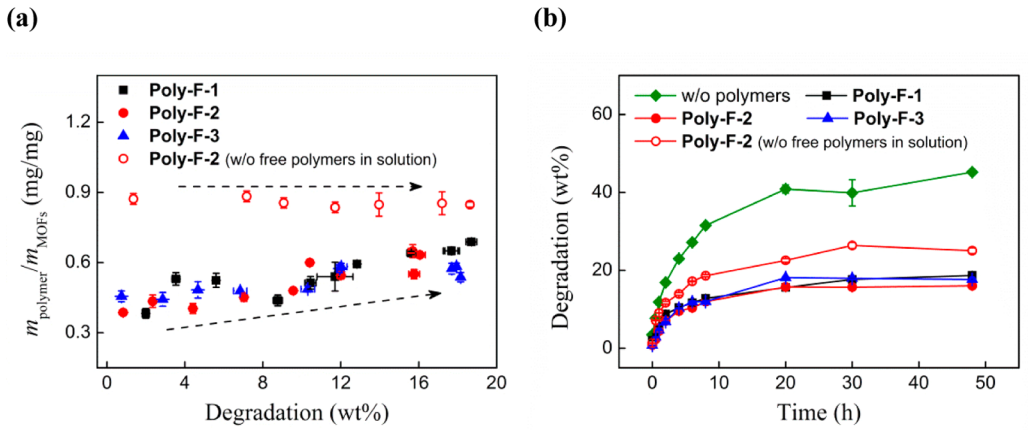

Figure 4. (a) Variation trend of the content of polymers on the surface of MIL-101-NH_2 (Fe) (0.04 mg/mL) upon degradation in aqueous solution, determined by the ratio of the amount of surface-adsorbed polymer to the original amount of MIL-101-NH_2 (Fe) in solution: (filled square, filled circle, and filled triangle) concentration of polymer is 0.05 mg/mL; (hollow circle) original concentration of polymer is 0.5 mg/mL; free polymer in solution was completely removed by centrifugal washing before the degradation experiment. (b) Kinetics of the degradation of MIL-101-NH_2 (Fe) (0.04 mg/mL) with and without surface bound/assembled polymers in water. Data are presented as the mean ± SD (n = 3).

chemistry has the potential to be great for surface engineering of nano-MOFs.

It should be noted that the noncovalent surface coatings on nano-MOFs are probably subject to exchange or exfoliation in complex environments. However, the results presented here show that the surface bound molecular probes/polymers are absolutely nonsheddable in water, even when subjected to intensive washing cycles and during the process of degradation,

dx.doi.org/10.1021/am500192b | ACS Appl. Mater. Interfaces 2014, 6, 5404−5412

which makes possible, in combination with well-developed conjugate chemistry, further postmodifications. For example, it would be interesting to design polymers not only with high affinity to nano-MOFs surface but also with diverse functional groups through which the surface polymers can be easily cross-linked. Such a combination of noncovalent and covalent strategy would also provide a new avenue for further improving the stability of nano-MOFs in complex aqueous systems.

CONCLUSION

In summary, the synergy of noncovalent interactions on the surface of MIL-101-NH_2 (Fe) has been systematically studied. We demonstrated that molecular probes with negative charges and hydrophobic property can bind and assemble on the MIL-101-NH_2 (Fe) surface with high affinity through synergistic noncovalent interactions and a process of cooperative binding. Functionalized polymers bearing surface binding moieties (side chain **F**) can bind effectively and quasi-permanently on the surface of MIL-101-NH_2 (Fe) in aqueous solution, even during the process of degradation, reflecting an achievement of manipulating the synergy of multiple noncovalent interactions as well as a favor from the dynamic features. The results presented herein constitute an important innovation for surface engineering of nano-MOFs, which should promote the development of porous nano-MOF based materials for multifunctional applications. In addition, our strategy should have the potential to be combined with known covalent conjugation strategy to decorate the surface of nano-MOFs with diverse new functions and properties.

MATERIALS AND METHODS

Preparation of MIL-101-NH_2 (Fe) Nanoparticles. Nanoscale MIL-101-NH_2 (Fe) was synthesized according to a previously reported procedure.[15] $FeCl_3 \cdot 6H_2O$ (135 mg, 0.5 mmol) and 2-aminoterephthalic acid (**L**, 90.5 mg, 0.5 mmol) were suspended in 25 mL of water and placed in a pressure reaction vial. The vial was kept at 60 °C for 10 min under microwave irradiation at 150 W. The obtained dark brown precipitate was recovered by centrifugation at 12 000 rpm for 20 min. After that, the precipitate was washed with ethanol by centrifugation and redispersed several times to remove the free reactants. An amount of 4 mg of the purified MIL-101-NH_2 (Fe) particles was then dispersed in 10 mL of ethanol for further use.

Synthesis of L-F and Poly-F-1/2/3. The details of the synthesis procedures and the characterization can be found in the Supporting Information.

Binding of Fluorescent Probes to MIL-101-NH_2 (Fe). Typically, to 0.475 mL of water was added 25 μL of MIL-101-NH_2 (Fe) (0.4 mg/mL) dispersed in ethanol. Then, 0.5 mL of 5 μM or 50 μM **L-F** (or **F**, **R**, and **P**) dissolved in water was added to the above MIL-101-NH_2 (Fe) solution, and the mixture was stirred at room temperature for around 10 min. After that, the particles were recovered from the mixture by centrifugation at 12 000 rpm for 20 min. Subsequently, 0.1 mL of the supernatant was taken out and diluted with an appropriate amount of phosphate buffer (10 mM, pH 7.4) for quantitative fluorescence measurement. The binding efficiency of the fluorescent probes to MIL-101-NH_2 (Fe) particles can then be determined by the molar ratio (n_f/n_L) of the bound probes to the **L** in MIL-101-NH_2 (Fe), which can be calculated through the following equation:

$$\frac{n_{\mathbf{f}}}{n_{\mathbf{L}}} = \frac{C_{\mathbf{f}(t)} - C_{\mathbf{f}(s)}}{C_{\mathbf{L}(t)}}$$

where $C_{f(t)}$ is the total concentration of fluorescent probes (i.e., 2.5 or 25 μM) in the incubation solution, $C_{L(t)}$ is the total concentration of **L** in suspension determined by fluorescence (**L** displays a strong fluorescence in the wavelength region of 400−500 nm under an excitation wavelength of 330 nm in phosphate buffer) when the dissolved MIL-101-NH_2 (Fe) particles were digested by phosphate buffer (10 mM, pH 7.4), $C_{f(s)}$ is the concentration of fluorescent probes that remained in the supernatant after the centrifugal precipitation of MIL-101-NH_2 (Fe) particles. Alternatively, the (n_f/n_L) can be obtained through measurement of the concentrations of fluorescent probes and **L** in the MIL-101-NH_2 (Fe) precipitate that was recovered by centrifugation. The MIL-101-NH_2 (Fe) precipitate can be completely digested to release **L** through dispersing in phosphate buffer.

Degradation of MIL-101-NH_2 (Fe). A 0.2 mL aqueous solution of MIL-101-NH_2 (Fe) (0.4 mg/mL) was added to 1.8 mL of water, and the solution was incubated at 37 °C. At a predefined time, aliquots were taken out and centrifuged at 12 000 rpm for 20 min. The concentration of ligand **L** in the supernatant can then be determined by fluorescence, which represents the extent of degradation of MIL-101-NH_2 (Fe) particles in aqueous solution.

Binding of L-F/F to MIL-101-NH_2 (Fe) in Degradation. An amount of 25 μL of MIL-101-NH_2 (Fe) (0.4 mg/mL) dispersed in ethanol was first diluted with 0.475 mL of water, to which 0.5 mL of aqueous solution of **L-F** (50 or 100 μM) or **F** (100 μM) was added, and the mixture was incubated at 37 °C for different time periods. At each time point, the solution was centrifuged at 12 000 rpm for 20 min, and the supernatant was taken out and diluted with 10 mM phosphate buffer (pH 7.4) to measure the fluorescence of free **L** and **L-F/F** in the solution. The concentration of free **L** and **L-F/F** remaining in the solution can then be obtained by fluorescence measurements. The molar ratio (n_f/n_L) of the bound **L-F/F** to the **L** in MIL-101-NH_2 (Fe) particles can then be calculated by this equation:

$$\frac{n_{\mathbf{f}}}{n_{\mathbf{L}}} = \frac{C_{\mathbf{f}(t)} - C_{\mathbf{f}(s)}}{C_{\mathbf{L}(t)} - C_{\mathbf{L}(s)}}$$

where $C_{f(t)}$ and $C_{L(t)}$ are the initial concentration of **L-F/F** (25 or 50 μM) and the total concentration of **L** in the mixture, respectively, and $C_{f(s)}$ and $C_{L(s)}$ are the concentrations of **L-F/F** and **L** in the supernatant (i.e., the unbound **L-F/F** and **L** that were released from the degraded particles).

Binding of Poly-F-1/2/3 to MIL-101-NH_2 (Fe). To 1.8 mL of water containing different concentrations of polymers (see Figure 3a), a 0.2 mL aqueous solution (0.4 mg/mL) of MIL-101-NH_2 (Fe) was added. The mixture was stirred for 10 min at room temperature and then was centrifuged at 12 000 rpm for 20 min, from which 0.1 mL of the supernatant was taken out and diluted with phosphate buffer (10 mM, pH 7.4) to measure the fluorescence intensity of free polymers remaining in solution. The amount of the polymers bound/assembled on the surface of MIL-101-NH_2 (Fe) can then be determined by the mass ratio (i.e., $m_{polymer}/m_{MOFs}$) of polymer to MIL-101-NH_2 (Fe) in precipitates through the following equation:

$$\frac{m_{\text{polymer}}}{m_{\text{MOFs}}} = \frac{C_{\text{polymer}(t)} - C_{\text{polymer}(s)}}{C_{\text{MOFs}(t)}}$$

where $C_{polymer(t)}$ and $C_{polymer(s)}$ are the total mass concentration of polymers in the incubation mixture and that in the supernatant, respectively, $C_{MOFs(t)}$ is the total mass concentration of MIL-101-NH_2 (Fe) particles in the mixture.

Binding of Control Polymers to MIL-101-NH_2 (Fe). An amount of 25 mg of polymers that are the homologues (**Poly-1/2/3**, without the conjugation of side chain **F**) of **Poly-F-1/2/3** and 20 mg of particles were added to 5 mL of water, and the mixture was stirred for 15 min. The mixture was centrifuged at 12 000 rpm for 20 min to precipitate the particles. The precipitated particles were then repeatedly washed with water 4 times. After that, the particles were digested by adding 10 mL of NaOH aqueous solution (0.1 M). The digestion solution was centrifuged to remove the digested precipitate, and 8 mL of the supernatant was taken out in which the excess NaOH was neutralized by adding HCl. The solvent of the supernatant was removed in vacuo, and the recovered residue was characterized by ^1H NMR. In order to determine the amount of control polymers in the residue, 5 μL of DMF was added as internal standard. As a contrast, an amount of 25 mg of

dx.doi.org/10.1021/am500192b | ACS Appl. Mater. Interfaces 2014, 6, 5404−5412

polymers that was dissolved in 5 mL of water was prepared from which 4 mL of the solution was taken for quantitative ^{1}H NMR measurement. It is worth mentioning that both the concentration of control polymers and MIL-101-NH_2 (Fe) used in this experiment are 100-fold higher than that used for probing the binding of **Poly-F-1/2/3** to MIL-101-NH_2 (Fe) (see Figure 3a) in order to afford a detectable signal from ^{1}H NMR measurements.

Reversibility of the Binding of Poly-F-1/2/3 to MIL-101-NH_2 (Fe). An amount of 1 mL of MIL-101-NH_2 (Fe) (0.4 mg/mL) in water and a 0.5 mL aqueous solution of **Poly-F-1/2/3** (10 mg/mL) were added to 3.5 mL of water. The mixture was stirred for 15 min. After centrifugation, the precipitated particles were redispersed in 1 mL of water, from which 0.2 mL of the solution was diluted by adding 1.8 mL of water. The sample was repeatedly centrifuged, decanted, and redispersed with water several times. After each centrifugation, the supernatant was recovered and added into an appropriate amount of phosphate buffer (10 mM, pH 7.4) for fluorescence measurements. The amount of polymers bound on the surface of MIL-101-NH_2 (Fe) can then be obtained by subtracting the amount of polymers remaining in the supernatant from the amount of polymers initially adsorbed on the particle surface.

Degradation of Polymer-Assembled MIL-101-NH_2 (Fe). To an aqueous solution (1.8 mL) containing 0.08 mg of MIL-101-NH_2 (Fe), 0.2 mL of **Poly-F-1/2/3** in water (0.5 mg/mL) was added. The mixture was incubated at 37 °C for different time periods. At predefined time points, the incubation solution was centrifuged at 12 000 rpm for 20 min, and 0.4 mL of the supernatant was collected and diluted with phosphate buffer (10 mM, pH 7.4) in order to measure the concentration of free **Poly-F-1/2/3** and **L** remaining in the solution. The amount of **Poly-F-1/2/3** bound/assembled on the surface of MIL-101-NH_2 (Fe) as the degradation proceeded can be obtained by this equation:

$$\frac{m_{\text{polymer}}}{m_{\text{MOFs}}} = \frac{C_{\text{polymer(t)}} - C_{\text{polymer(s)}}}{C_{\text{MOFs(t)}}}$$

where $C_{\text{polymer(t)}}$ and $C_{\text{polymer(s)}}$ are the total mass concentration of polymers in the incubation mixture and that in the supernatant, respectively, and $C_{\text{MOFs(t)}}$ is the initial mass concentration of MIL-101-NH_2 (Fe) in the mixture.

In the case of probing the degradation of **Poly-F-2** bound/assembled MIL-101-NH_2 (Fe) while free polymers in solution that were not bound on the particle surface were completely removed by centrifugal washing, 2.5 mL of aqueous solution of MIL-101-NH_2 (Fe) (0.4 mg/mL) and 1.25 mL of **Poly-F-2** dissolved in water (10 mg/mL) were mixed and added to 6.25 mL of water. The mixture was then stirred for 15 min and centrifuged to recover the particles. The recovered particles were redispersed in 2.5 mL of water, from which 0.2 mL of the solution (0.2 mg/mL) was added to 1.8 mL of water. The degradation was then monitored as described above.

Preparation of Sample for TGA and IR Absorption Spectroscopy. To an aqueous solution (3.0 mL) containing 20 mg of MIL-101-NH_2 (Fe) was added 10 mg of polymer (**Poly-F-2**). The mixture was incubated at 37 °C for 10 min. After that, the solution was centrifuged at 11 000 rpm for 10 min. The precipitated particles were then washed with water once. After drying under vacuum at 50 °C overnight, the sample was characterized by TGA and IR absorption spectroscopy.

■ ASSOCIATED CONTENT

Ⓢ Supporting Information

Figures S1−S18, Tables S1−S3, details of the synthesis and characterization of **L-F** and **Poly-F-1/2/3**, and supplementary materials and methods. This material is available free of charge via the Internet at http://pubs.acs.org.

■ AUTHOR INFORMATION

Corresponding Author

*E-mail: chlwu@xmu.edu.cn.

Author Contributions

S.L. and C.W. conceived the study, designed the experiments, and analyzed results. S.L., L.Z., C.L., and Y.L. performed the experiments. All authors contributed to the writing of the manuscript.

Notes

The authors declare no competing financial interest.

■ ACKNOWLEDGMENTS

We acknowledge the financial support of the National Basic Research 973 Program of China (Grant 2014CB932004) and the National Natural Science Foundation of China (Grant 21305114 and 21375110). We also thank Xiaojing Zhao for experimental help.

■ REFERENCES

(1) Eddaoudi, M.; Moler, D. B.; Li, H.; Chen, B.; Reineke, T. M.; O'Keeffe, M.; Yaghi, O. M. Modular Chemistry: Secondary Building Units as a Basis for the Design of Highly Porous and Robust Metal−Organic Carboxylate Frameworks. *Acc. Chem. Res.* **2001**, *34* (4), 319−330.

(2) Férey, G. Hybrid Porous Solids: Past, Present, Future. *Chem. Soc. Rev.* **2008**, *37* (1), 191−214.

(3) Férey, G.; Mellot-Draznieks, C.; Serre, C.; Millange, F. Crystallized Frameworks with Giant Pores: Are There Limits to the Possible? *Acc. Chem. Res.* **2005**, *38* (4), 217−225.

(4) Cui, Y.; Yue, Y.; Qian, G.; Chen, B. Luminescent Functional Metal−Organic Frameworks. *Chem. Rev.* **2011**, *112* (2), 1126−1162.

(5) Getman, R. B.; Bae, Y.-S.; Wilmer, C. E.; Snurr, R. Q. Review and Analysis of Molecular Simulations of Methane, Hydrogen, and Acetylene Storage in Metal−Organic Frameworks. *Chem. Rev.* **2011**, *112* (2), 703−723.

(6) Kreno, L. E.; Leong, K.; Farha, O. K.; Allendorf, M.; Van Duyne, R. P.; Hupp, J. T. Metal−Organic Framework Materials as Chemical Sensors. *Chem. Rev.* **2011**, *112* (2), 1105−1125.

(7) Li, J.-R.; Sculley, J.; Zhou, H.-C. Metal−Organic Frameworks for Separations. *Chem. Rev.* **2011**, *112* (2), 869−932.

(8) Suh, M. P.; Park, H. J.; Prasad, T. K.; Lim, D.-W. Hydrogen Storage in Metal−Organic Frameworks. *Chem. Rev.* **2011**, *112* (2), 782−835.

(9) Sumida, K.; Rogow, D. L.; Mason, J. A.; McDonald, T. M.; Bloch, E. D.; Herm, Z. R.; Bae, T.-H.; Long, J. R. Carbon Dioxide Capture in Metal−Organic Frameworks. *Chem. Rev.* **2011**, *112* (2), 724−781.

(10) Wu, H.; Gong, Q.; Olson, D. H.; Li, J. Commensurate Adsorption of Hydrocarbons and Alcohols in Microporous Metal Organic Frameworks. *Chem. Rev.* **2012**, *112* (2), 836−868.

(11) Yoon, M.; Srirambalaji, R.; Kim, K. Homochiral Metal−Organic Frameworks for Asymmetric Heterogeneous Catalysis. *Chem. Rev.* **2011**, *112* (2), 1196−1231.

(12) Della Rocca, J.; Liu, D.; Lin, W. Nanoscale Metal−Organic Frameworks for Biomedical Imaging and Drug Delivery. *Acc. Chem. Res.* **2011**, *44* (10), 957−968.

(13) Horcajada, P.; Gref, R.; Baati, T.; Allan, P. K.; Maurin, G.; Couvreur, P.; Férey, G.; Morris, R. E.; Serre, C. Metal−Organic Frameworks in Biomedicine. *Chem. Rev.* **2011**, *112* (2), 1232−1268.

(14) Taylor-Pashow, K. M. L.; Rocca, J. D.; Xie, Z.; Tran, S.; Lin, W. Postsynthetic Modifications of Iron-Carboxylate Nanoscale Metal−Organic Frameworks for Imaging and Drug Delivery. *J. Am. Chem. Soc.* **2009**, *131* (40), 14261−14263.

(15) Horcajada, P.; Chalati, T.; Serre, C.; Gillet, B.; Sebrie, C.; Baati, T.; Eubank, J. F.; Heurtaux, D.; Clayette, P.; Kreuz, C.; Chang, J.-S.; Hwang, Y. K.; Marsaud, V.; Bories, P.-N.; Cynober, L.; Gil, S.; Ferey, G.; Couvreur, P.; Gref, R. Porous Metal-Organic-Framework Nanoscale Carriers as a Potential Platform for Drug Delivery and Imaging. *Nat. Mater.* **2010**, *9* (2), 172−178.

(16) Kitagawa, S.; Kitaura, R.; Noro, S.-i. Functional Porous Coordination Polymers. *Angew. Chem., Int. Ed.* **2004**, *43* (18), 2334−2375.

(17) Férey, G.; Serre, C. Large Breathing Effects in Three-Dimensional Porous Hybrid Matter: Facts, Analyses, Rules and Consequences. *Chem. Soc. Rev.* **2009**, *38* (5), 1380−1399.
(18) Miller, S. R.; Heurtaux, D.; Baati, T.; Horcajada, P.; Greneche, J.-M.; Serre, C. Biodegradable Therapeutic MOFs for the Delivery of Bioactive Molecules. *Chem. Commun.* **2010**, *46* (25), 4526−4528.
(19) Hinks, N. J.; McKinlay, A. C.; Xiao, B.; Wheatley, P. S.; Morris, R. E. Metal Organic Frameworks as NO Delivery Materials for Biological Applications. *Microporous Mesoporous Mater.* **2010**, *129* (3), 330−334.
(20) Baati, T.; Njim, L.; Neffati, F.; Kerkeni, A.; Bouttemi, M.; Gref, R.; Najjar, M. F.; Zakhama, A.; Couvreur, P.; Serre, C.; Horcajada, P. In Depth Analysis of the in Vivo Toxicity of Nanoparticles of Porous Iron(III) Metal-Organic Frameworks. *Chem. Sci.* **2013**, *4* (4), 1597−1607.
(21) Alexis, F.; Pridgen, E.; Molnar, L. K.; Farokhzad, O. C. Factors Affecting the Clearance and Biodistribution of Polymeric Nanoparticles. *Mol. Pharm.* **2008**, *5* (4), 505−515.
(22) Gupta, A. K.; Gupta, M. Synthesis and Surface Engineering of Iron Oxide Nanoparticles for Biomedical Applications. *Biomaterials* **2005**, *26* (18), 3995−4021.
(23) Win, K. Y.; Feng, S.-S. Effects of Particle Size and Surface Coating on Cellular Uptake of Polymeric Nanoparticles for Oral Delivery of Anticancer Drugs. *Biomaterials* **2005**, *26* (15), 2713−2722.
(24) Rowe, M. D.; Thamm, D. H.; Kraft, S. L.; Boyes, S. G. Polymer-Modified Gadolinium Metal-Organic Framework Nanoparticles Used as Multifunctional Nanomedicines for the Targeted Imaging and Treatment of Cancer. *Biomacromolecules* **2009**, *10* (4), 983−993.
(25) Huxford, R. C.; deKrafft, K. E.; Boyle, W. S.; Liu, D.; Lin, W. Lipid-Coated Nanoscale Coordination Polymers for Targeted Delivery of Antifolates to Cancer Cells. *Chem. Sci.* **2012**, *3* (1), 198−204.
(26) Liu, D.; Kramer, S. A.; Huxford-Phillips, R. C.; Wang, S.; Della Rocca, J.; Lin, W. Coercing Bisphosphonates to Kill Cancer Cells with Nanoscale Coordination Polymers. *Chem. Commun.* **2012**, *48* (21), 2668−2670.
(27) Huxford-Phillips, R. C.; Russell, S. R.; Liu, D.; Lin, W. Lipid-Coated Nanoscale Coordination Polymers for Targeted Cisplatin Delivery. *RSC Adv.* **2013**, *3* (34), 14438−14443.
(28) Liu, D.; Huxford, R. C.; Lin, W. Phosphorescent Nanoscale Coordination Polymers as Contrast Agents for Optical Imaging. *Angew. Chem., Int. Ed.* **2011**, *50* (16), 3696−3700.
(29) Rieter, W. J.; Pott, K. M.; Taylor, K. M. L.; Lin, W. Nanoscale Coordination Polymers for Platinum-Based Anticancer Drug Delivery. *J. Am. Chem. Soc.* **2008**, *130* (35), 11584−11585.
(30) Taylor, K. M. L.; Rieter, W. J.; Lin, W. Manganese-Based Nanoscale Metal−Organic Frameworks for Magnetic Resonance Imaging. *J. Am. Chem. Soc.* **2008**, *130* (44), 14358−14359.
(31) Rieter, W. J.; Taylor, K. M. L.; Lin, W. Surface Modification and Functionalization of Nanoscale Metal-Organic Frameworks for Controlled Release and Luminescence Sensing. *J. Am. Chem. Soc.* **2007**, *129* (32), 9852−9853.
(32) deKrafft, K. E.; Boyle, W. S.; Burk, L. M.; Zhou, O. Z.; Lin, W. Zr- and Hf-Based Nanoscale Metal-Organic Frameworks as Contrast Agents for Computed Tomography. *J. Mater. Chem.* **2012**, *22* (35), 18139−18144.
(33) Rowe, M. D.; Chang, C.-C.; Thamm, D. H.; Kraft, S. L.; Harmon, J. F.; Vogt, A. P.; Sumerlin, B. S.; Boyes, S. G. Tuning the Magnetic Resonance Imaging Properties of Positive Contrast Agent Nanoparticles by Surface Modification with RAFT Polymers. *Langmuir* **2009**, *25* (16), 9487−9499.
(34) Cunha, D.; Ben Yahia, M.; Hall, S.; Miller, S. R.; Chevreau, H.; Elkaïm, E.; Maurin, G.; Horcajada, P.; Serre, C. Rationale of Drug Encapsulation and Release from Biocompatible Porous Metal−Organic Frameworks. *Chem. Mater.* **2013**, *25* (14), 2767−2776.
(35) Canivet, J.; Aguado, S.; Schuurman, Y.; Farrusseng, D. MOF-Supported Selective Ethylene Dimerization Single-Site Catalysts through One-Pot Postsynthetic Modification. *J. Am. Chem. Soc.* **2013**, *135* (11), 4195−4198.
(36) Horcajada, P.; Serre, C.; Vallet-Regí, M.; Sebban, M.; Taulelle, F.; Férey, G. Metal−Organic Frameworks as Efficient Materials for Drug Delivery. *Angew. Chem., Int. Ed.* **2006**, *45* (36), 5974−5978.
(37) Horcajada, P.; Serre, C.; Maurin, G.; Ramsahye, N. A.; Balas, F.; Vallet-Regí, M.; Sebban, M.; Taulelle, F.; Férey, G. Flexible Porous Metal-Organic Frameworks for a Controlled Drug Delivery. *J. Am. Chem. Soc.* **2008**, *130* (21), 6774−6780.
(38) Kondo, M.; Furukawa, S.; Hirai, K.; Kitagawa, S. Coordinatively Immobilized Monolayers on Porous Coordination Polymer Crystals. *Angew. Chem., Int. Ed.* **2010**, *49* (31), 5327−5330.
(39) Lacerda, S. H. D. P.; Park, J. J.; Meuse, C.; Pristinski, D.; Becker, M. L.; Karim, A.; Douglas, J. F. Interaction of Gold Nanoparticles with Common Human Blood Proteins. *ACS Nano* **2009**, *4* (1), 365−379.
(40) De La Cruz, E. M. Cofilin Binding to Muscle and Non-Muscle Actin Filaments: Isoform-Dependent Cooperative Interactions. *J. Mol. Biol.* **2005**, *346* (2), 557−564.
(41) Ikeda, Y.; Taniguchi, N.; Noguchi, T. Dominant Negative Role of the Glutamic Acid Residue Conserved in the Pyruvate Kinase M1 Isozyme in the Heterotropic Allosteric Effect Involving Fructose-1,6-bisphosphate. *J. Biol. Chem.* **2000**, *275* (13), 9150−9156.
(42) Jain, P. K.; Huang, W.; El-Sayed, M. A. On the Universal Scaling Behavior of the Distance Decay of Plasmon Coupling in Metal Nanoparticle Pairs: A Plasmon Ruler Equation. *Nano Lett.* **2007**, *7* (7), 2080−2088.
(43) Averick, S.; Simakova, A.; Park, S.; Konkolewicz, D.; Magenau, A. J. D.; Mehl, R. A.; Matyjaszewski, K. ATRP under Biologically Relevant Conditions: Grafting from a Protein. *ACS Macro Lett.* **2011**, *1* (1), 6−10.
(44) Cheng, G.; Zhang, Z.; Chen, S. F.; Bryers, J. D.; Jiang, S. Y. Inhibition of Bacterial Adhesion and Biofilm Formation on Zwitterionic Surfaces. *Biomaterials* **2007**, *28* (29), 4192−4199.
(45) Lutz, J. F.; Stiller, S.; Hoth, A.; Kaufner, L.; Pison, U.; Cartier, R. One-Pot Synthesis of PEGylated Ultrasmall Iron-Oxide Nanoparticles and Their in Vivo Evaluation as Magnetic Resonance Imaging Contrast Agents. *Biomacromolecules* **2006**, *7* (11), 3132−3138.
(46) Ma, H.; Li, D.; Sheng, X.; Zhao, B.; Chilkoti, A. Protein-Resistant Polymer Coatings on Silicon Oxide by Surface-Initiated Atom Transfer Radical Polymerization. *Langmuir* **2006**, *22* (8), 3751−3756.
(47) Trmcic-Cvitas, J.; Hasan, E.; Ramstedt, M.; Li, X.; Cooper, M. A.; Abell, C.; Huck, W. T. S.; Gautrot, J. E. Biofunctionalized Protein Resistant Oligo(ethylene glycol)-Derived Polymer Brushes as Selective Immobilization and Sensing Platforms. *Biomacromolecules* **2009**, *10* (10), 2885−2894.
(48) Wang, X. S.; Armes, S. P. Facile Atom Transfer Radical Polymerization of Methoxy-Capped Oligo(ethylene glycol) methacrylate in Aqueous Media at Ambient Temperature. *Macromolecules* **2000**, *33* (18), 6640−6647.
(49) Giljohann, D. A.; Seferos, D. S.; Daniel, W. L.; Massich, M. D.; Patel, P. C.; Mirkin, C. A. Gold Nanoparticles for Biology and Medicine. *Angew. Chem., Int. Ed.* **2010**, *49* (19), 3280−3294.
(50) Kievit, F. M.; Zhang, M. Q. Surface Engineering of Iron Oxide Nanoparticles for Targeted Cancer Therapy. *Acc. Chem. Res.* **2011**, *44* (10), 853−862.
(51) Lee, D. E.; Koo, H.; Sun, I. C.; Ryu, J. H.; Kim, K.; Kwon, I. C. Multifunctional Nanoparticles for Multimodal Imaging and Theragnosis. *Chem. Soc. Rev.* **2012**, *41* (7), 2656−2672.
(52) Mout, R.; Moyano, D. F.; Rana, S.; Rotello, V. M. Surface Functionalization of Nanoparticles for Nanomedicine. *Chem. Soc. Rev.* **2012**, *41* (7), 2539−2544.
(53) Zrazhevskiy, P.; Sena, M.; Gao, X. H. Designing Multifunctional Quantum Dots for Bioimaging, Detection, and Drug Delivery. *Chem. Soc. Rev.* **2010**, *39* (11), 4326−4354.
(54) Liu, W.-L.; Lo, S.-H.; Singco, B.; Yang, C.-C.; Huang, H.-Y.; Lin, C.-H. Novel Trypsin-FITC@MOF Bioreactor Efficiently Catalyzes Protein Digestion. *J. Mater. Chem. B* **2013**, *1* (7), 928−932.